Development of a new correlation to calculate permeability for flows with high Knudsen number

Esmaeil Dehdashti†

Department of Mechanical Engineering, University of Tehran, Tehran 515-14395, *Iran*

(Received 1 June 2015; revised manuscript received 12 August 2015; published online 20 December 2015)

Flows with high Knudsen number play a prominent role in many engineering applications. The present study is an effort toward the simulation of flow with high Knudsen number using modified lattice Boltzmann method (LBM) through a porous medium in a channel. The effect of collision between molecules and solid walls, which is required to accurately simulate transition flow regime, is taken into account using a modified relaxation time. Slip velocity on the wall, which is another significant difficulty in simulating transition flow regime, is captured using the slip reflection boundary condition (SRBC). The geometry of porous medium is considered as in-line and staggered. The results are in good agreement with previous works. A new correlation is obtained between permeability, Knudsen number and porosity for flows in transition flow regimes.

Keywords: flow in porous micro-channel, lattice Boltzmann method, high Knudsen number, permeability

PACS: 47.61.−k, 07.10.Cm, 47.61.Fg, 81.40.−z **DOI:** 10.1088/1674-1056/25/2/024702

1. Introduction

Due to the recent rapid development of micro flow devices applied in micro-total-analysis-systems (m-TAS) and micro-electro-mechanical systems (MEMS),[1–5] modeling and simulation methods for flows in such micro geometries have been of great interest in the society of computational physics.[6–8] In many mathematical models of important phenomena with real-life applications, one faces the challenge of spatial scales. This is true in particular in the study of flow and transport in porous media, which is important in environmental studies, geophysics, reservoir engineering, and medicine.

Flow through the porous medium has become one of the most significant research subjects in many science and engineering fields because of its wide spectrum of applications. In particular, the prediction of macroscopic or effective transport properties has been considered as a fundamental and practical problem.[9] Advances in micromachining technology have spawned many opportunities to precisely fabricate mechanical devices of micron size such as channels, nozzles, and so forth.

The Navier–Stokes (macroscopic momentum) equations are, no longer applicable to flows with high Knudsen number and the physics of flow in such flows is described by the Boltzmann equation (BE) of the gas kinetic theory.[10] For example, problems such as multiphase flows,[11] turbulent flow,[12,13] flows considering fluid–solid interaction (FSI),[14] and thermal flow[15] could be handled effectively using the LBM. For $Kn < 10^{-3}$ the continuity assumption with no slip boundary conditions is valid. For $10^{-3} < Kn < 10^{-1}$ (slip flow regime) the velocity and temperature of the gas near the wall are no longer equal to the wall velocity and temperature respectively and for $Kn > 10^{-1}$ (transition and free molecular flow regime) the continuity assumption is under question.[6] For the transition regime ($Kn > 10^{-1}$), the continuity assumption and consequently the validity of the Navier–Stokes equations, NSE, is questionable as the size is reduced significantly. In such cases, because of the solid walls effect, the fluid flow behavior depends strongly on the geometry dimensions.[6]

Recently there have been efforts to employ the LBM for flows with high Knudsen number in slip flow regime[16–22] but only a few papers can be mentioned for the use of LBM in transition regime.[23–29] To this end, two methods are proposed based on the use of higher order LBM[23–26] and the modification of the mean free path.[26–29] The multi-speed or higher order LBM has been developed to increase the order of accuracy in the discretization of velocity phase space. Although Ansumali, *et al.*[25] have demonstrated that the high-order LBMs have improved current capability, Kim *et al.*[26] showed that this method can predict the rarefaction effects only for $Kn = O(0.1)$ and at large Kn, the mass flow rate cannot be predicted properly by these methods. Additionally, the high-order LBMs with large numbers of discrete velocities are not numerically stable.[30] One of the problems which happens in the high Kn number flow in a channel is that velocity profiles of flow in the transition and free molecular regimes remain approximately parabolic. But the velocity profile obtained from continuum-based relations does not predict the flow rate properly.[6] This is due to the fact that the dynamic viscosity must be modified to consider the diffusion of momentum because of the intermolecular collisions and the col-

†Corresponding author. E-mail: iman.dehdashti@ut.ac.ir

© 2016 Chinese Physical Society and IOP Publishing Ltd

lision of molecules with the walls in comparison to considering the diffusion of momentum because of the intermolecular collisions alone. In the transition regime, intermolecular collisions and molecule–wall collisions have the same order, while in the free molecular regime, the molecule–wall collisions are the dominant phenomenon. However, to the best of our knowledge, there were few efforts to study and find a correlation between permeability, porosity, and Knudsen number in the transition regime.

In the present study, we first simulate flows through a channel with low Knudsen number. A porous medium, which is considered as in-line and staggered, is placed through the channel. A schematic picture of two kinds of geometry is shown in Fig. 1 and Fig. 2. The flow with Knudsen number up to 10 is simulated and a new correlation is achieved between permeability, porosity, and Knudsen number. Afterward, results for low Knudsen number are presented to show that our simulations are in good agreement with the previous results. Thereafter, results for transition flow are shown and a new relation was attained to calculate non-dimensional permeability as a function of porosity and Knudsen number. Our investigations can contribute significantly to our understanding of flow and change of properties in the transition regime.



Fig. 1. Solution domain including porous medium with in-line geometry.

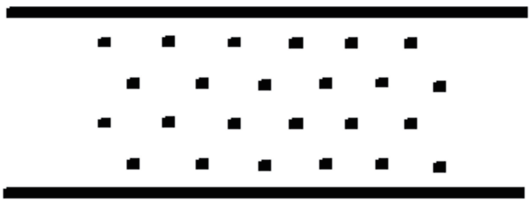


Fig. 2. Solution domain including porous medium with staggered geometry.

The rest of this paper is organized in the following way. The formulations for LBM are presented in Section 2. Thereafter, the modification required to solve flow with high Kn number is explained in Section 3. In Section 4, boundary conditions are presented. The results and respective discussions are given in Section 5. The conclusion and the future works which can be done as a continuation of this work are presented in Section 6.

2. Lattice Boltzmann method

The LBM originated from lattice gas (LG) automata,[31] which are discrete particle kinetics based on discrete time and lattice spaces. The LB equation is expressed as:

$$f_i(\boldsymbol{x}+\boldsymbol{e}_i\Delta t, t+\Delta t) - f_i(\boldsymbol{x},t) = \Omega_i(f(\boldsymbol{x},t)) \tag{1}$$

where $f_i(\boldsymbol{x},t)$ denotes the probability of finding a particle at lattice site $\boldsymbol{x}$ and time t, which moves with the local particle velocity $\boldsymbol{e}_i$. Furthermore, Δt is the time increment, and Ω_i is the collision operator for the rate of change of f_i resulting from collision, and it depends only on the local value of $f_i(\boldsymbol{x},t)$.

In Eq. (1), the local particle velocity $\boldsymbol{e}_i$ is discrete in the given lattice. For a D2Q9 lattice model, the discrete velocities for the nine possible directions are:

$$\begin{aligned} e_0 &= 0, \\ e_i &= \left[\cos\left(\frac{((i-1)\pi)}{2}\right), \sin\left(\frac{((i-1)\pi)}{2}\right)\right] c, \quad i = 1 \sim 4, \\ e_i &= \left[\cos\left(\frac{((i-1)\pi)}{2} + \frac{\pi}{4}\right), \sin\left(\frac{((i-1)\pi)}{2} + \frac{\pi}{4}\right)\right] \sqrt{2}c, \\ & \qquad\qquad i = 5 \sim 8, \end{aligned}$$

where $c = \Delta x/\Delta t$ and Δx is the lattice spacing step.

For the BGK model,[32] the collision operator is expressed as:

$$\Omega_i = -\frac{f_i(\boldsymbol{x},t) - f_i^{(\mathrm{eq})}(\boldsymbol{x},t)}{\tau},$$

where τ is the relaxation time and $f_i^{(eq)}$ denotes the local equilibrium distribution, which is defined as:

$$f_i^{(\mathrm{eq})} = \rho w_i \left(1 + \frac{e_{ik}u_k}{c_s^2} + \frac{(e_{ik}u_k)^2}{2c_s^4} - \frac{u_k u_k}{2c_s^2}\right), \tag{2}$$

in which ρ is the fluid density, u is the fluid velocity, $c_s = c/\sqrt{3}$ is the lattice speed of sound. Where weight coefficients in Eq. (2) are as follows:

$$\begin{aligned} w_0 &= \frac{4}{9}; \\ w_i &= \frac{1}{9}, \qquad i = 1-4; \\ w_i &= \frac{1}{36}, \qquad i = 5-8. \end{aligned}$$

The fluid density ρ and momentum density $\rho\boldsymbol{u}$ are expressed as:

$$\rho = \sum_{i=0}^{8} f_i, \qquad \rho\boldsymbol{u} = \sum_{i=0}^{8} \boldsymbol{e}_i f_i.$$

Furthermore, it can be shown that the pressure fluid p and the kinematic viscosity ν derived from the Boltzmann BGK equation through the Chapman–Enskog expansion is

$$p = c_s^2\rho, \qquad \nu = \Delta t c_s^2(\tau - 0.5).$$

In equilibrium, the conservation of mass and momentum is satisfied at each lattice

$$\sum_{i=0}^{8} \Omega_i = 0, \qquad \sum_{i=0}^{8} \Omega_i \boldsymbol{e}_i = 0.$$

3. LBM for high Knudsen number flows

It is found out from the direct simulation Monte Carlo (DSMC) method and linearized Boltzmann equation[33] that velocity profiles in a channel in transition and free molecular regimes remain roughly parabolic. But the velocity profile which is obtained from relations based on continuum assumption does not predict the flow rate properly.[6] This is due to the fact that any discrete velocity model describes a whole set of molecular speeds within a finite solid angle, by a single discrete speed. Although the reduction of degrees of freedom leads to a very efficient scheme, it causes the particles, which in fact collide with the wall, moving parallel to it and make an unrealistic free-acceleration regime due to the effect of pressure gradients or body forces within the fluid flow.[34] Therefore, a general form of the effective viscosity as a function of the Knudsen number has been proposed,[6] which is valid for a wide range of flow regimes

$$\mu_{\text{eff}} = \frac{\mu}{1+f(Kn)}.$$

Pollard and Present[35] proposed a rather simple model for generalized diffusion coefficient which sets $f(Kn) = \alpha Kn$. Karniadakis and Beskok[6] suggested the value $\alpha = 2.2$ in their effort to match their numerical results for the mass flow rate in a channel with the corresponding DSMC results. To model the rarefaction effect in the transition regime, kinematic viscosity is modified as given below

$$\nu_{\text{eff}} = \frac{\mu_{\text{eff}}}{\rho_{\text{eff}}} = \nu\left(\frac{1}{1+f(Kn)}\frac{\rho}{\rho_{\text{eff}}}\right).$$

One should note that U and ρ in Eq. (12) are the macroscopic kinematic viscosity and density of the fluid, whereas the quantities with the "eff" subscript represent the effective values at the particular Knudsen number. Considering the effective viscosity and density, we have defined a new effective relaxation time in the LBM as follows:

$$\tau_{\text{eff}} = 0.5 + \left(\frac{1}{1+f(Kn)}\frac{\rho}{\rho_{\text{eff}}}\right)(\tau - 0.5),$$

where $\tau = 0.5 + \sqrt{6/\pi}KnH$ is the non-dimensional relaxation time and H is a characteristic length (e.g. height of the micro channel).[36]

4. Boundary conditions in LBM

In the present work, since flow with high Kn number is simulated, it is required to apply a boundary condition on solid walls to be capable of predicting the slip velocity on solid walls. The boundary condition which is applied to fulfill the required conditions on solid walls is the slip reflection boundary condition (SRBC),[37] which is a combination of the bounce back and specular boundary conditions. For example, at the lower boundaries, the unknown particle distribution functions f_2, f_5, and f_6, can be calculated as follows:

$$\begin{bmatrix} f_5(x,0) \\ f_2(x,0) \\ f_6(x,0) \end{bmatrix} = \begin{bmatrix} s & 0 & 1-s \\ 0 & 1 & 0 \\ 1-s & 0 & s \end{bmatrix} \begin{bmatrix} f_7(x+\delta x, \delta y) \\ f_4(x,\delta y) \\ f_8(x-\delta x,\delta y) \end{bmatrix}, \quad (3)$$

where s is the slip-reflection coefficient on the solid wall. In Eq. (3), one obtains the bounce back boundary condition when $s = 1$ and specular boundary condition when $s = 0$. Equilibrium boundary condition is employed in inlet and outlet.

5. Results and discussion

In the present study, two-dimensional flow in a channel is solved. Moreover, there is a porous medium, which is considered in-line and staggered, through the channel. In this section, non-dimensional permeability (k/d^2) is calculated in different conditions including different Kn and porosity (ϵ). To validate the results, flow with low Kn is simulated, then we extend high Kn and a new correlation is derived for transition flow regime.

First, the flow with low Kn number is solved in a channel. The results are compared to the those of Jeong *et al.*[9] for low Kn number. Our study shows that for low Kn number, changes of Kn number do not have a noticeable influence on the results.

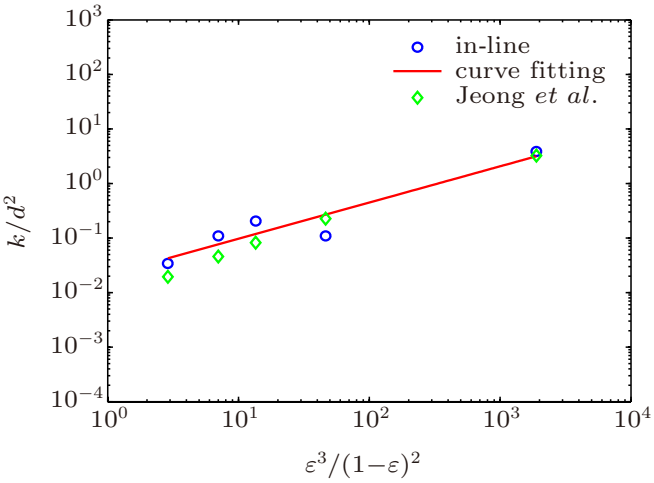


Fig. 3. (color online) Non-dimensional permeability versus porosity for in-line geometry.

Figures 3 and 4 show our results for a single Kn number with both in-line and staggered structures. It is evident that there is a good agreement between the present results and those obtained by Jeong *et al.*[9] We then solve the flow with high Kn in a channel. To insure that our results for high Kn number are correct, slip boundary condition for flow with high Kn number must be validated, besides the relaxation time, which was validated by the results in Fig. 3 and Fig. 4. To

validate slip boundary condition velocity profile in the channel flow without presence of porous medium is simulated. The results are shown in Figs. 5 and 6. It is evident that SRBC can satisfactorily predict slip velocity on the walls. The figures show a good agreement between the present results and those attained by linearized Boltzmann equation.

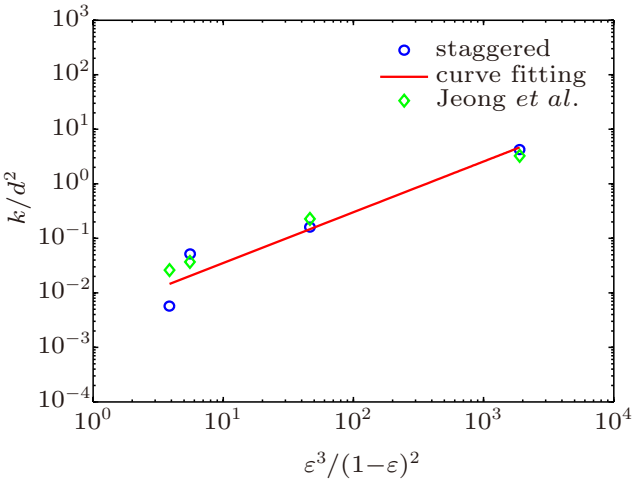


Fig. 4. (color online) Non-dimensional permeability versus porosity for staggered geometry.

After validating the boundary condition and the relaxation time, flow with high Kn number through a channel through which a porous medium placed is solved. The investigations show that non-dimensional permeability depends on porosity and Kn number. So, the following simulations will be performed to achieve a new correlation between k/d^2, ϵ, and Kn. First, as shown in Fig. 7, k/d^2 versus $\epsilon^3/(1-\epsilon)^2$ is represented for different Kn number in a channel through which an in-line porous medium is placed. It is shown that non-dimensional permeability increases when the simulation is performed for flow with higher porosity, which is a reasonable result based on the concept of permeability and porosity. Our results also show that non-dimensional permeability is changed with different Kn numbers. This triggers a motivation to find a correlation between non-dimensional permeability, porosity, and Kn number. To achieve the correlation, non-dimensional permeability is considered as a function of porosity, that is,

$$k/d^2 = A(\epsilon^3/(1-\epsilon)^2)^B,$$

its coefficients can be obtained by fitting curves to the results for different Kn numbers, as shown in Fig. 7. Thus, both coefficients of A and B are calculated for diverse Kn numbers and given in Table 1. To obtain a correlation, which indicates the non-dimensional permeability versus porosity and Kn number, it is required to determine both coefficients as functions of Kn number. Hence, the coefficients, as shown in Fig. 8, were determined by fitting a second order polynomial (A (or B) $= C_1Kn^2 + C_2Kn + C_3$) to the results. The amounts of C_1, C_2, and C_3 are shown in Table 2. Therefore, the new correlation between non-dimensional permeability, porosity, and Kn number are given below

$$\frac{k}{d^2} = (-0.003619Kn^2 + 0.06016Kn + 0.1855) \times \left(\frac{\epsilon^3}{(1-\epsilon)^2}\right)^{(0.0005306Kn^2 - 0.008453Kn + 0.569)}. \quad (4)$$

Table 1. A and B for flows with different Kn numbers in a channel through which an in-line porous medium is placed.

Kn	1	4	7	10
A	0.2362	0.3856	0.4118	0.4309
B	0.5624	0.5399	0.5397	0.5363

Table 2. The amounts of C_1, C_2, and C_3 for flow in a channel through which an in-line porous medium is placed.

	C_1	C_2	C_3
A	−0.003619	0.06016	0.1855
B	0.0005306	−0.008453	0.569

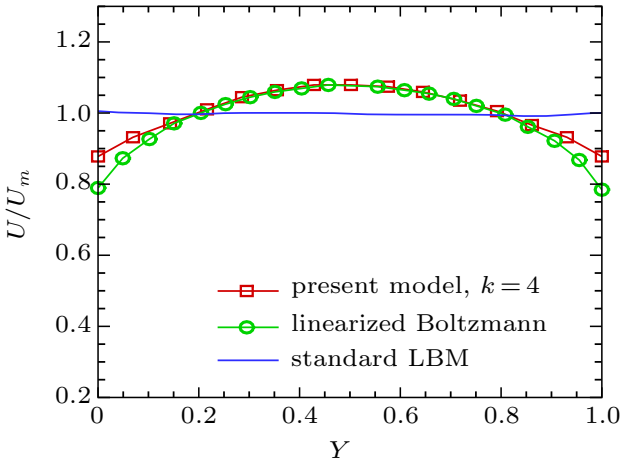


Fig. 5. (color online) Velocity profile for flow through a channel at K which is defined as $\sqrt{\pi}/2Kn$ equal to 4.

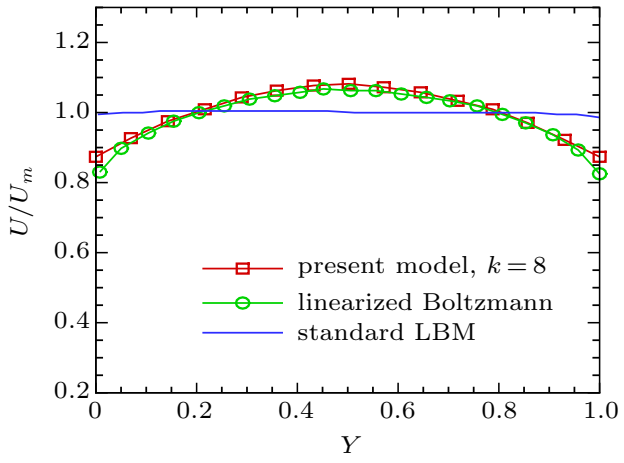


Fig. 6. (color online) Velocity profile for flow through a channel at K which is defined as $\sqrt{\pi}/2Kn$ equal to 8.

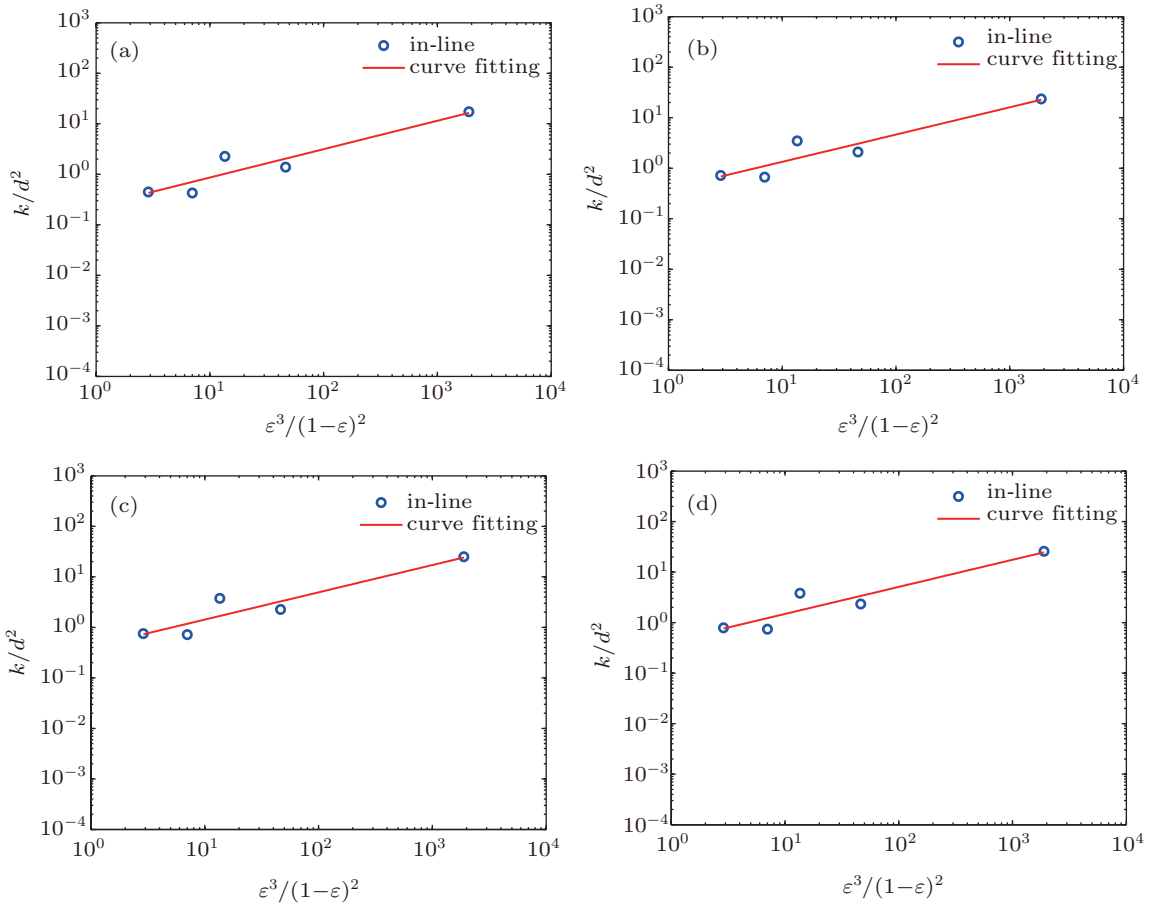


Fig. 7. (color online) Non-dimensional permeability versus porosity for in-line geometry and different Kn number: (a) $Kn = 1$, (b) $Kn = 4$, (c) $Kn = 7$, and (d) $Kn = 10$.

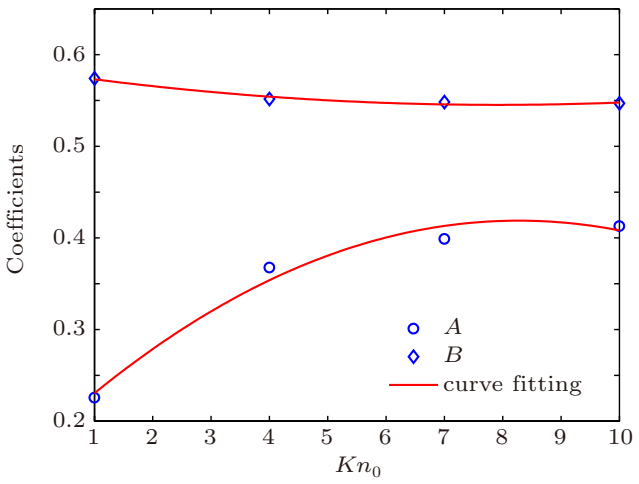


Fig. 8. (color online) A and B for flows with different Kn numbers in a channel through which an in-line porous medium is placed.

Now that the results are shown for in-line porous medium, those for a staggered porous medium are shown in the following to assess whether or not geometry of porous medium has a significant influence on results. Hence, we investigate the flow in a channel through which a staggered porous medium is placed. The results are shown in Fig. 9. It is discernible that the results have the same trend as those of in-line geometry (Fig. 7). Moreover, A and B are calculated as shown in Table 3. It is evident that the coefficients are near to those of in-line geometry (Table 1). In view of similarity between A and B, non-dimensional permeability with respect to porosity of staggered porous medium changes in a way similar to those of in-line one. Moreover, both coefficients are to determine how they change with different Kn numbers. As shown in Fig. 10 a second-order curve is fitted to each of the results of A and B for different Kn numbers. Table 4 indicates the values of C_1, C_2, and C_3, from which one can deduce that the results are similar to those of in-line geometry (Table 2). Hence, the correlation for geometry of staggered medium is as follows:

$$\frac{k}{d^2} = (-0.003619Kn^2 + 0.05889Kn + 0.1752) \times \left(\frac{\epsilon^3}{(1-\epsilon)^2}\right)^{(0.0005833Kn^2 - 0.009237Kn + 0.5818)}. \tag{5}$$

All in all, it can be concluded from what was mentioned above, that there is not the strong reliance between non-dimensional permeability and the geometry of porous medium. Hence, it is reasonable to consider non-dimensional permeability as a function of porosity and Kn number.

Table 3. A and B for flows with different Kn numbers in a channel through which a staggered porous medium is placed.

Kn	1	4	7	10
A	0.2259	0.3677	0.3992	0.4129
B	0.5740	0.5516	0.5483	0.5469

Table 4. The amounts of C_1, C_2, and C_3 for flow in a channel through which a staggered porous medium is placed.

	C_1	C_2	C_3
A	−0.003558	0.05889	0.1752
B	0.0005833	−0.009237	0.5818

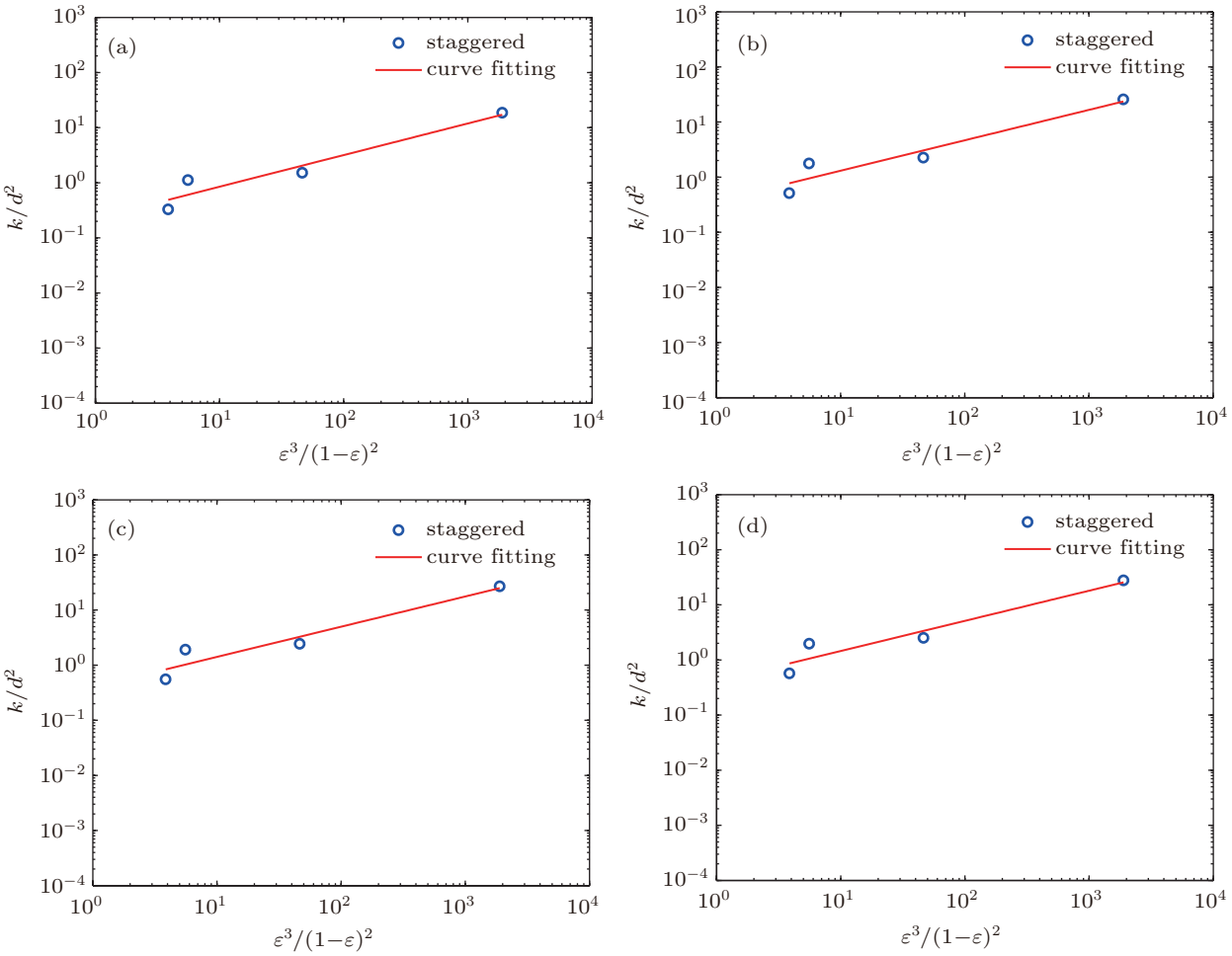


Fig. 9. (color online) Non-dimensional permeability versus porosity for staggered geometry and different Kn number: (a) $Kn = 1$, (b) $Kn = 4$, (c) $Kn = 7$, and (d) $Kn = 10$.

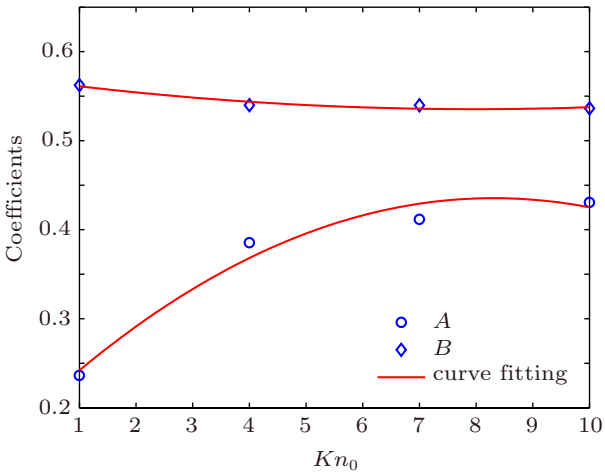


Fig. 10. (color online) A and B for flows with different Kn numbers in a channel through which a staggered porous medium is placed.

6. Conclusion

In the present study, flow was solved in a channel in which a porous medium exists. Results are presented for both in-line and staggered geometries of the porous medium. Since changes of porosity and Kn number do not influence the non-dimensional permeability of flow with low Kn number, the results are presented for a single Kn number. Thereafter, simulation was extended to flow with high Kn number up to 10. SRBC was employed to capture slip velocity on the walls in flow with high Kn number. Moreover, an appropriate relaxation time was applied to simulate rarefied flows. The results show that the non-dimensional permeability is strongly dependent on porosity and Kn number in flow with high Kn number. Since it was also illustrated that non-dimensional permeability is not strongly dependent on geometry of porous medium, a

correlation was derived between non-dimensional permeability, porosity, and *Kn* number. Nonetheless, the correlation was obtained for in-line and staggered geometry. The present study is a promising work to calculate permeability as a function of porosity and *Kn* number. This work can be seminal to future research on understanding and developing new methods to study rarefied flows. Also, the present work can be extended to more complex problems such as FSI, flow in a more complex geometry and so forth.

References

[1] Dehrouyeh-Semnani A M and Nikkhah-Bahrami M 2014 *Composite Structures* **122** 425
[2] Dehrouyeh-Semnani A M and Nikkhah-Bahrami M 2015 *Int. J. Eng. Sci.* **86** 20
[3] Dehrouyeh-Semnani A M and Nikkhah-Bahrami M 2015 *Composite Structures* **123** 325
[4] Mohammad-Abadi M and Daneshmehr A 2015 *Int. J. Eng. Sci.* **87** 83
[5] Mohammad-Abadi M and Daneshmehr A 2014 *Int. J. Eng. Sci.* **75** 40
[6] Karniadakis G, Beskok A and Aluru N 2006 *Microows and Nanoows: Fundamentals and Simulation* (New York: Springer)
[7] Salem A M, Ismail G and Fathy R 2014 *Chin. Phys. B* **23** 044402
[8] Song H Q, Yu M X, Zhu W Y, Zhang Y and Jiang S X 2013 *Chin. Phys. Lett.* **30** 14701
[9] Namgyun J, Hyung C D and Ching-Long L 2006 *Journal of Micromechanics and Microengineering* **16** 2240
[10] Suga K, Takenaka S, Ito T and Kaneda M 2010 *Journal of Micromechanics and Microengineering* **2** 609
[11] Swift M R, Orlandini E, Osborn W R and Yeomans J M 1996 *Phys. Rev. E* **54** 5041
[12] Soe M, Vahala G, Pavlo P, Vahala L and Chen H 1998 *Phys. Rev. E* **57** 4227
[13] Chai Z H, Shi B C and Zheng L 2006 *Chin. Phys.* **15** 1855
[14] Kwon Y 2006 *Eng. Comp.* **23** 860
[15] Peng Y, Shu C and Chew Y T 2003 *Phys. Rev. E* **68** 026701
[16] Agrawal A, Djenidi L and Antonia R 2005 *J. Fluid Mech.* **530** 135
[17] Guo Z and Zhao T and Shi Y 2006 *J. Appl. Phys.* **99** 074903
[18] Guo Z, Shi B, Zhao T and Zheng C 2007 *Phys. Rev. E* **76** 056704
[19] Guo Z, Zheng C and Shi B 2008 *Phys. Rev. E* **77** 036707
[20] Kim W T, Jhon M S, Zhou Y, Staroselsky I and Chen H 2005 *J. Appl. Phys.* **97** 304
[21] Lee T and Lin C L 2005 *Phys. Rev. E* **71** 046706
[22] Verhaeghe F, Luo L S and Blanpain B 2009 *J. Comput. Phys.* **228** 147
[23] Shan X W, Yuan X F and Chen H D 2006 *J. Fluid Mech.* **550** 413
[24] Chikatamarla S S and Karlin I V 2006 *Phys. Rev. Lett.* **97** 190601
[25] Ansumali S, Karlin I V, Arcidiacono S, Abbas A and Prasianakis N 2007 *Phys. Rev. Lett.* **98** 124502
[26] Kim S H, Pitsch H and Boyd I D 2008 *J. Comput. Phys.* **227** 8655
[27] Zhang Y H, Gu X J, Barber R W and Emerson D R 2006 *Phys. Rev. E* **74** 046704
[28] Zhang Y H, Tang G and Emerson D R 2008 *Phys. Rev. E* **77** 046701
[29] Tang G H, Zhang Y H, Gu X J and Emerson D R 2008 *Europhys. Lett.* **83** 40008
[30] Succi S, Karlin I V and Chen H 2002 *Rev. Mod. Phys.* **74** 1203
[31] Pomeau B H Y and Frisch U 1986 *Phys. Rev. Lett.* **56** 1505
[32] Bhatnagar P L, Gross E P and Krook M 1954 *Phys. Rev.* **94** 511
[33] Ohwada T, Sone Y and Aoki K 1989 *Physics of Fluids A: Fluid Dynamics* **1** 2042
[34] Toschi F and Succi S 2005 *Europhys. Lett.* **69** 549
[35] Pollard W G and Present R D 1948 *Phys. Rev.* **73** 762
[36] Nie X, Doolen G D and Chen S 2002 *J. Stat. Phys.* **107** 279
[37] Succi S 2002 *Phys. Rev. Lett.* **89** 064502